SCHOOL OF CHEMICAL ENGINEERING

THE UNIVERSITY of ADELAIDE

# Supporting Information

## Optically Optimized Photoluminescent and Interferometric Biosensors Based on Nanoporous Anodic Alumina: A Comparison

**Abel Santos, Tushar Kumeria and Dusan Losic***

School of Chemical Engineering, The University of Adelaide, SA 5005, Australia

Losic Group

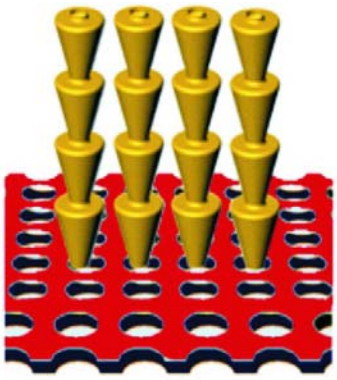

NanoTech Research

## S1. Fabrication Conditions and Geometric Characteristics of NAA platforms

NAA platforms were fabricated by anodizing aluminum (Al) foils by the two-step process. After fabrication, the geometric characteristics of these NAA platforms (i.e. the pore length and its diameter) were established by SEM images acquired through a scanning electron microscope (FEG-SEM FEI Quanta 450), which were subsequently analyzed by the standard image processing package ImageJ (public domain program developed at the RSB of the NIH). The fabrication conditions and the geometric characteristics of the different NAA platforms are summarized in **Table S1** and **Figure S1**.

| | | $t_{pw}$ (min) | | | | |
|---|---|---|---|---|---|---|
| **($L_p$ ; $d_p$)** (μm ; nm) | | 0 | 4 | 8 | 12 | 16 |
| $t_{an}$ (h) | 0.5 | (1.8±0.2 ; 29±2) | (1.8±0.2 ; 40±2) | (1.8±0.2 ; 47±2) | (1.8±0.2 ; 55±2) | (1.8±0.2 ; 64±2) |
| | 1.0 | (3.6±0.2 ; 29±2) | (3.6±0.2 ; 40±2) | (3.6±0.2 ; 47±2) | (3.6±0.2 ; 55±2) | (3.6±0.2 ; 64±2) |
| | 1.5 | (5.3±0.3 ; 29±2) | (5.3±0.3 ; 40±2) | (5.3±0.3 ; 47±2) | (5.3±0.3 ; 55±2) | (5.3±0.3 ; 64±2) |
| | 2.0 | (6.4±0.4 ; 29±2) | (6.4±0.4 ; 40±2) | (6.4±0.4 ; 47±2) | (6.4±0.4 ; 55±2) | (6.4±0.4 ; 64±2) |
| | 2.5 | (8.4±0.2 ; 29±2) | (8.4±0.2 ; 40±2) | (8.4±0.2 ; 47±2) | (8.4±0.2 ; 55±2) | (8.4±0.2 ; 64±2) |

**Table S1.** Anodization conditions and geometric characteristics of the different NAA platforms used in this study.

Notice that, all these measurements were repeated three times at different parts of the NAA sample (i.e. cross-section and top view) and three different NAA samples were analyzed per geometric parameter (i.e. 9 measurements per geometric parameter and anodization conditions). Finally, the obtained values were statistically treated by calculating averages and experimental errors.

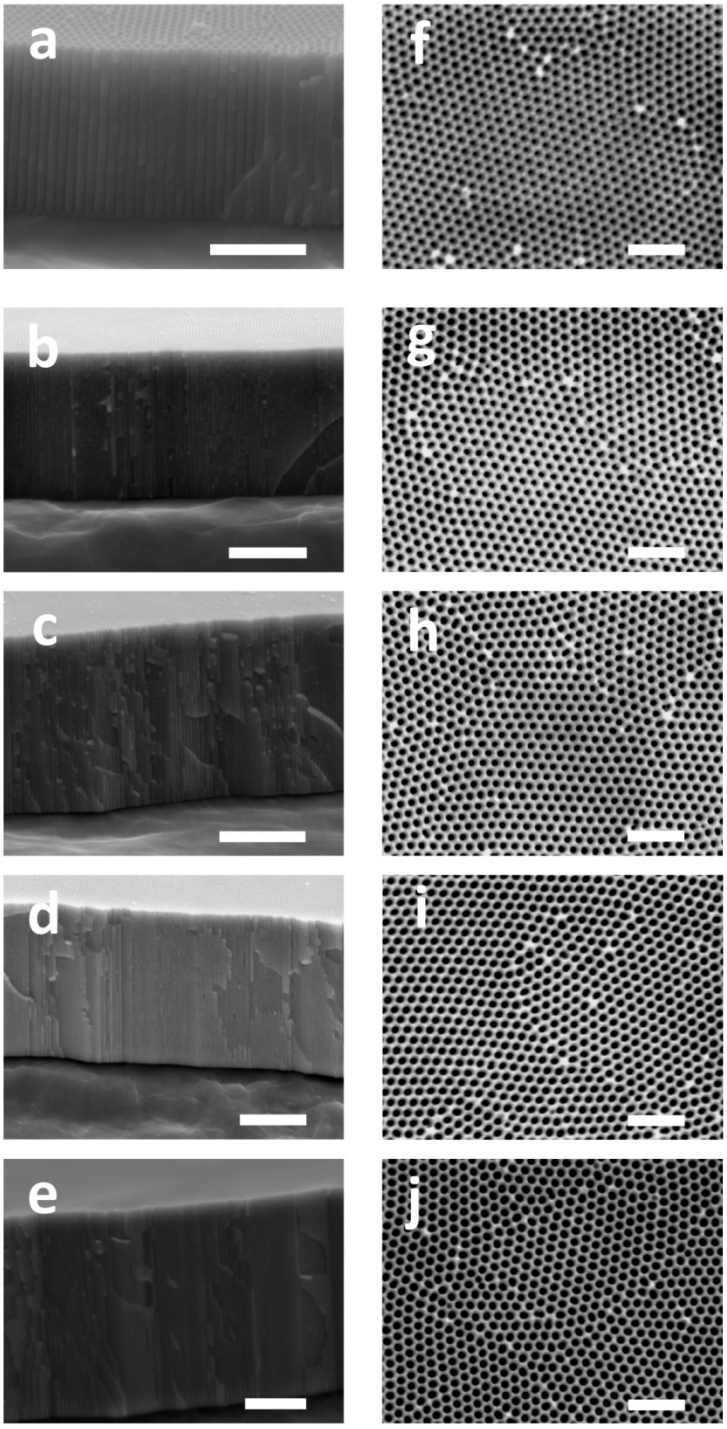


**Figure S1.** Set of SEM cross-section and top view images of NAA platforms featuring different pore lengths and diameters. a) $t_{an}$ = 0.5 h (scale bar = 1 μm). b) $t_{an}$ = 1.0 h (scale bar = 2 μm). c) $t_{an}$ = 1.5 h (scale bar = 2.5 μm). d) $t_{an}$ = 2.0 h (scale bar = 2.5 μm). e) $t_{an}$ = 2.5 h (scale bar = 2.5 μm). f) $t_{pw}$ = 0 min (scale bar = 500 nm). g) $t_{pw}$ = 4 min (scale bar = 500 nm). h) $t_{pw}$ = 8 min (scale bar = 500 nm). i) $t_{pw}$ = 12 min (scale bar = 500 nm). j) $t_{pw}$ = 16 min (scale bar = 500 nm).

## S2. Fluorescein Isothiocyanate (FITC) Visual Test

The functionalization process through the APTES-GTA protocol was validated through a fluorescein isothiocyanate (FITC) visual test reported elsewhere.[1] This was carried out by dipping two NAA platforms, one functionalized and the other one non-functionalized, into an aqueous solution of FITC 200 μg $mL^{-1}$ for 2 h at room temperature and subsequent washing with distilled water. **Figure S2** shows a digital photography of these NAA platforms. This reveals that the functionalized sample acquired a yellow tonality as a result of the FITC immobilization through the NAA pores with the activated APTES layer whereas the non-functionalized sample kept the characteristic transparent color of NAA fabricated in oxalic acid under mild anodization conditions.

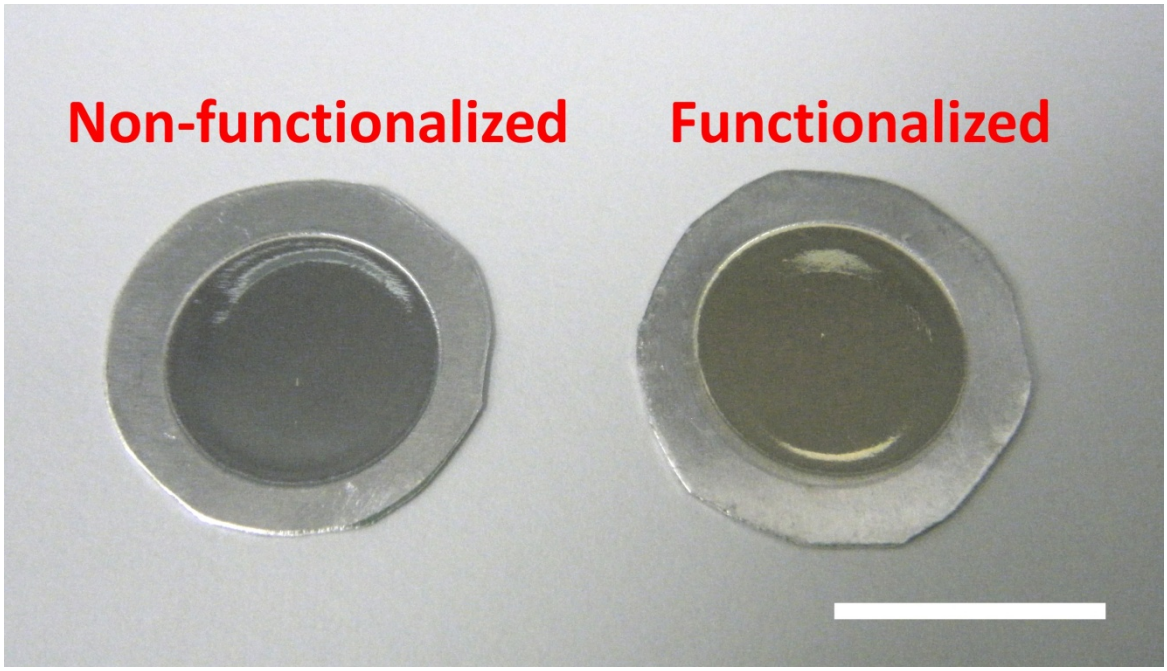


**Figure S2.** Digital photography of two NAA platforms functionalized and non-functionalized with APTES after the FITC visual test (scale bar = 1 cm).

## S3. Raw Data $OT_{eff}$ of and its Calculation

As an example, **Table S2** compiles the values of $OT_{eff}$ measured before and after detection of D-glucose in NAA platforms combined with PLS.

**D-Glucose in PLS-NAA under non-specific adsorption conditions**

| ***[Glucose]*** (M) | $OT_{eff-0}$ (nm) | $OT_{eff-f}$ (nm) | $\Delta OT_{eff}$ (nm) † | $\Delta OT_{eff}$ (%) |
|---|---|---|---|---|
| 0.01 | 4060.4 ± 1.9 | 4067.9 ± 1.6 | 7.5 ± 1.6 | 0.20 ± 0.04 |
| 0.05 | 4060.1 ± 1.5 | 4076.9 ± 1.2 | 16.8 ± 1.2 | 0.40 ± 0.03 |
| 0.10 | 4062.3 ± 4.2 | 4117.7 ± 4.1 | 55.4 ± 4.1 | 1.40 ± 0.10 |
| 0.20 | 4066.6 ± 2.2 | 4230.3 ± 21.2 | 163.7 ± 20.3 | 4.18 ± 0.50 |
| 0.55 | 4064.8 ± 1.4 | 4397.4 ± 16.2 | 332.6 ± 16.2 | 8.29 ± 0.40 |
| 1.20 | 4069.1 ± 2.1 | 4688.3 ± 12.2 | 619.2 ± 12.2 | 15.46 ± 0.30 |

**Table S2.** Raw data corresponding to the calculation of $\Delta OT_{eff}$ for detection of D-glucose under non-specific adsorption conditions in PLS-NAA sensing platforms (these values correspond are represented in **Figure 4a** of this manuscript). $OT_{eff-0}$ and $OT_{eff-f}$ indicate the effective optical thickness of these NAA platforms before and after adsorption of D-glucose molecules, respectively. †Calculated as: $\Delta OT_{eff} = \Delta OT_{eff-f} - \Delta OT_{eff-0}$.

Notice that $OT_{eff-0}$ is the effective optical thickness of the NAA platform without considering the angle of incidence (in this case 40°, as indicated in the manuscript for PLS). After applying **Equation 1**, we found that the obtained physical thickness of these samples (i.e. $L_p$ – pore length) was in good agreement with the estimation obtained from the calibration curves shown in **Figure 2** of this manuscript.

As a graphical example of these calculations, **Figure S3** shows the PLS and FFT spectra of NAA platforms used to detect D-glucose 1.20 M.

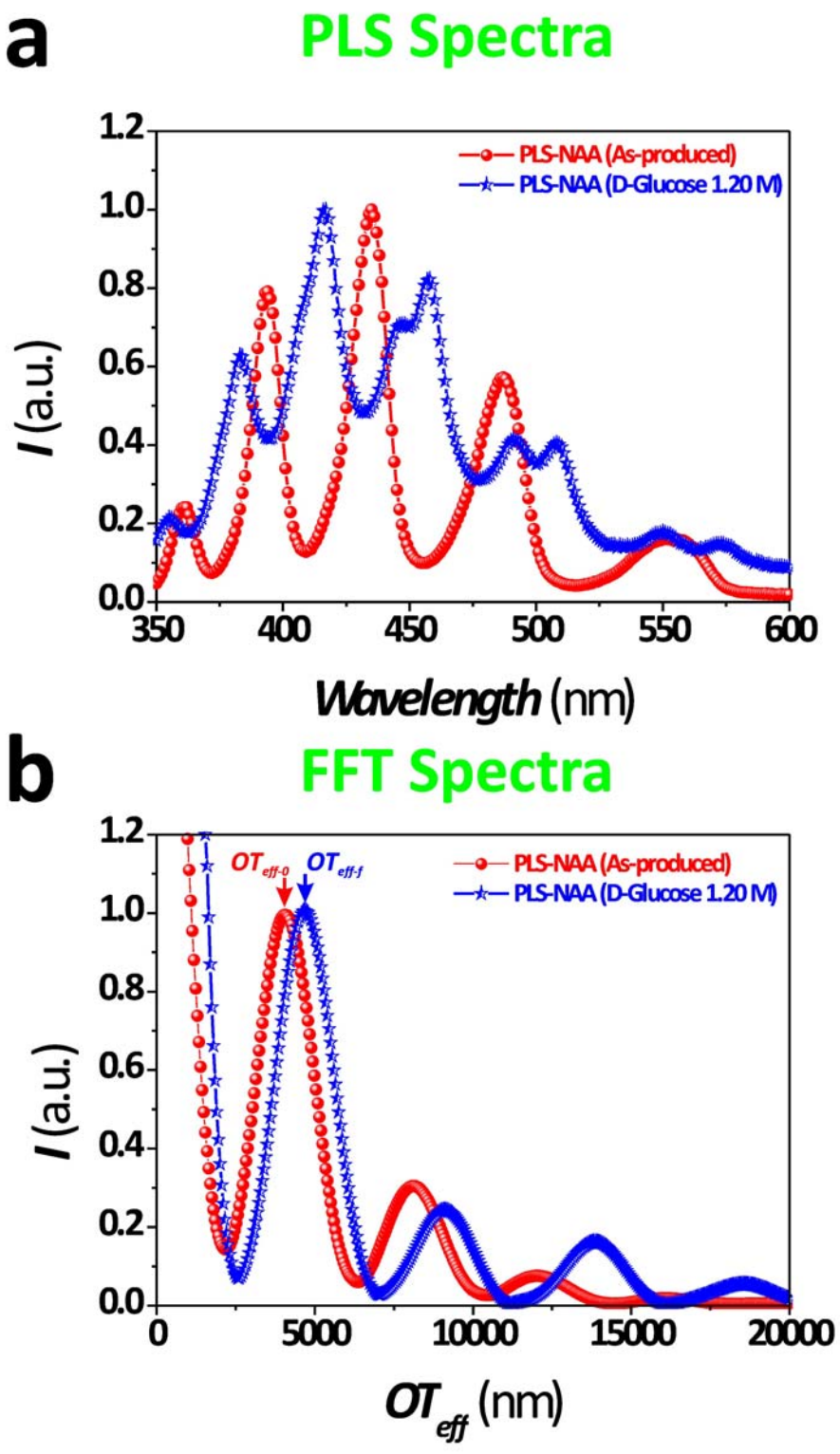


**Figure S3.** PLS and FFT spectra of NAA platforms used to detect D-glucose 1.20 M. a) PLS spectrum before and after adsorption of D-glucose. b) FFT spectrum before and after adsorption of D-glucose.

## S4. Fourier Transform IR (FTIR) Spectroscopy Analysis

Two NAA platforms infiltrated with aqueous solutions of D-glucose and L-cysteine 50 mM were analyzed through Fourier transform IR (FTIR) spectroscopy (**Figure S4**). To this end, the remaining aluminum substrate was removed from the NAA backside by wet chemical etching in a saturated solution of hydrochloric acid and cupric chloride (HCl / $CuCl_2$). Notice that the FTIR spectrum of as-produced NAA samples was used as a background. FTIR spectra were collected in a FTIR spectrometer (Nexus 6700 Nicolet ThermoFisher). The number of scans was set to 32 with a resolution of 4 $cm^{-1}$. All spectra were collected in the range 4000-1500 $cm^{-1}$ in transmission mode.

**Figure S4a** shows the FTIR spectrum of a NAA platform infiltrated with D-glucose under non-specific immobilization conditions. This shows a strong peak that corresponds to the bands from 2900 to 3450 $cm^{-1}$ assigned to CH and OH vibrational groups of D-glucose molecules.[2] **Figure S4b** shows the FTIR spectrum of a NAA platform infiltrated with L-cysteine under specific immobilization conditions. A strong peak is observed at around 2540 $cm^{-1}$ in the IR spectrum, which is associated with the SH stretching mode of L-cysteine molecules.[3]

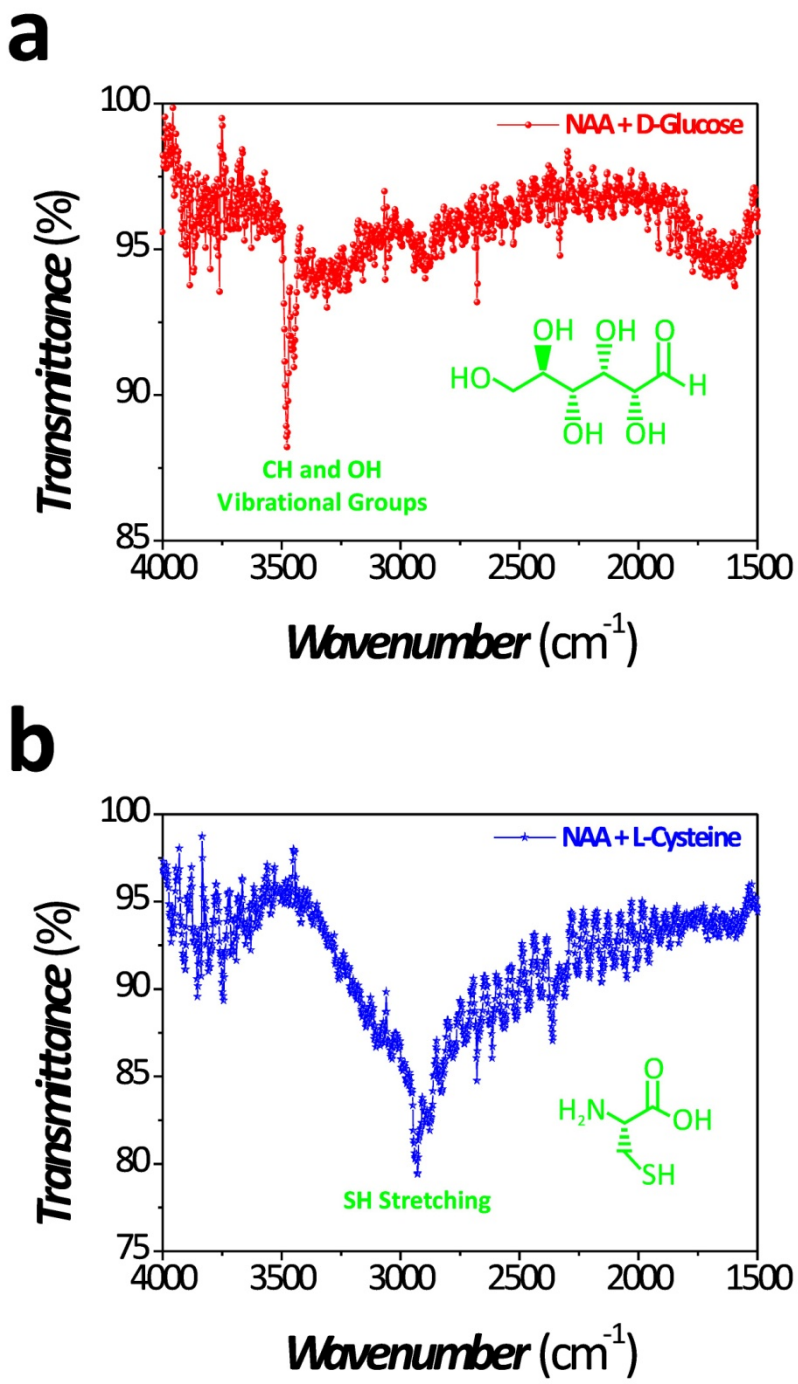


**Figure S4.** FTIR spectra of NAA platforms infiltrated with D-glucose 50 mM (a) and L-cysteine 50 mM (b) under specific and non-specific immobilization conditions.

## S5. Definition of Optical Parameter *OP*

The sensing parameter used in PLS-NAA and RIfS-NAA platforms is the effective optical thickness ($OT_{eff}$). This optical parameter makes it possible to establish the amount of analyte in the range of linear performance of these biosensors (i.e. range within which the effective optical thickness change is proportional to the analyte concentration). Therefore, to establish the most optimal NAA platform, we used the parameter *OP*, which is defined as the ratio between the maximum peak intensity and its width at half of the intensity value calculated from the FFT spectra obtained from the PLS and RIfS spectra (i.e. effective optical thickness peak). **Figure S5** shows the definition of this parameter, which was used to optimize the different sensing platforms analyzed in this study (i.e. PLS-NAA and RIfS-NAA).

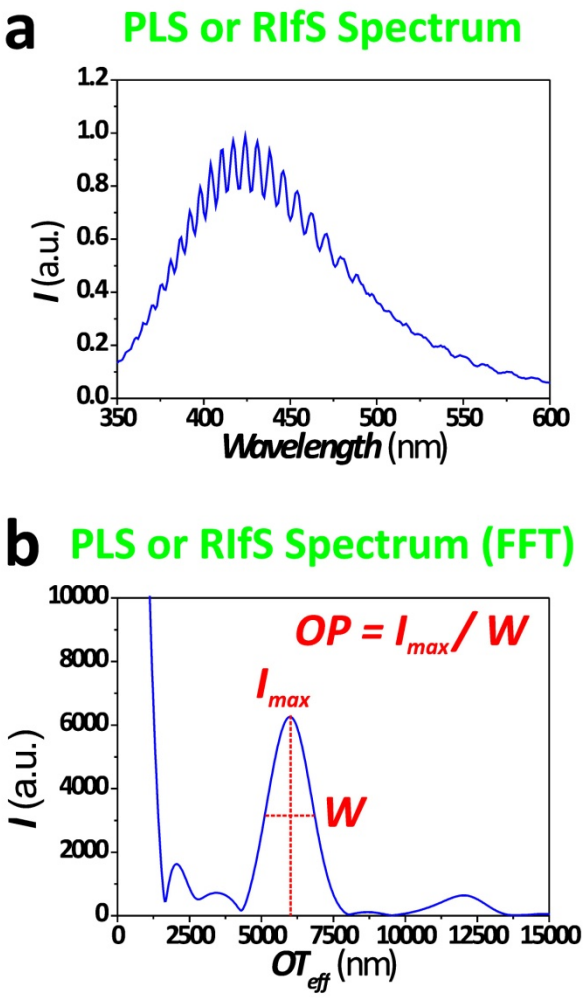


**Figure S5.** Definition of the parameter *OP* obtained from the PLS or RIfS spectrum (a) after applying the fast Fourier Transform (FFT) (b).

## S6. PLS and UV-visible Spectra of D-Glucose and L-Cysteine Solutions

The PLS and UV-visible spectra of two solutions of D-glucose and L-cysteine with the same analyte concentration (i.e. 50 mM) were acquired in order to study the optical properties of these analytes. PLS spectra were acquired in a spectrofluorometer (Fluoromax-4 Horiba Jobin Yvon) equipped with a Xe lamp used as the excitation light source at room temperature. The excitation wavelength ($\lambda_{ex}$) was set to 320 nm with a slit size of 5 nm. UV-visible spectra were acquired in a UV-visible spectrometer (Carry 60 spectrophotometer Agilent technologies). As **Figure S6a** shows, it was verified that D-glucose is much more photoluminescent than L-cysteine. Nevertheless, both solutions showed a very low and comparable absorbance in the wavelength range analyzed in this study (**Figure S6b**).

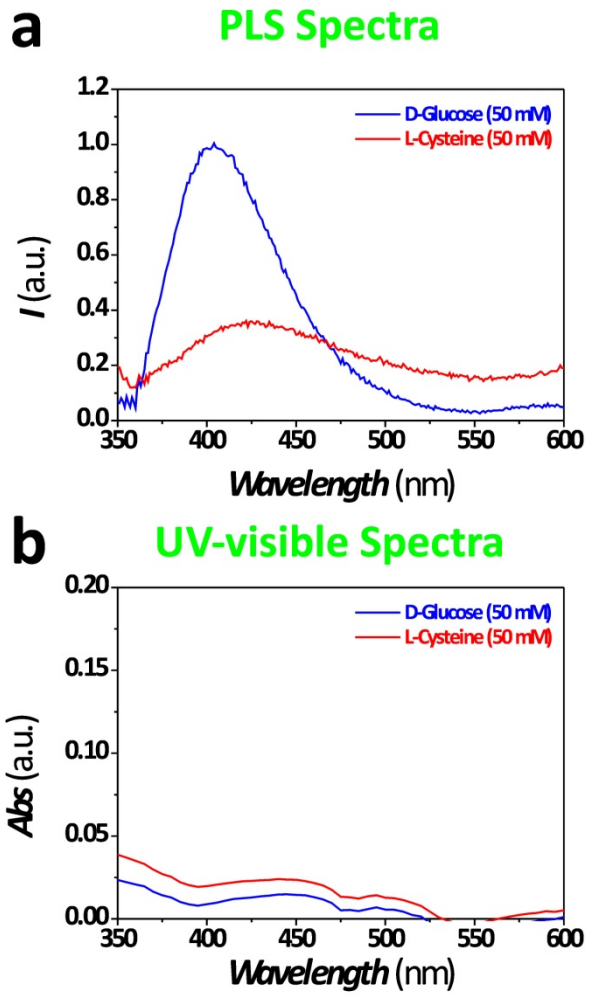


**Figure S6.** PLS (a) and UV-visible (b) spectra of aqueous solutions of D-Glucose and L-Cysteine 50 mM.

## References

(1) Md Jani, A. M.; Kempson, I. M.; Losic, D.; Voelcker, N. H. *Angew. Chem., Int. Ed.* **2010**, *49*, 7933−7937.

(2) Ibrahim, M.; Alaam, M.; El-Haes, H.; Jalbout, A. F.; de Leon, A. *Ecletica Quim.* **2006**, *31*, 15–21.

(3) Pawlukojc, A.; Leciejewicz, J.; Ramirez-Cuesta, A. J.; Nowicka-Scheibe, J. *Spectrochim. Acta, Part A* **2005**, *61*, 2474–2481.